Influence of Switching Conditions on the VFTO Magnitudes in a GIS

V. Vinod Kumar, Joy Thomas M., and M. S. Naidu

***Abstract*—Estimation of Very Fast Transient Overvoltage (VFTO) has been carried out using EMTP for various switching conditions in a 420 kV gas insulated substation. The variation of VFTO peak along the GIS bus nodes for disconnector and circuit breaker switching operations as well as the variation of VFTO peak with different magnitudes of trapped charges have been studied. The results indicate a distinct pattern of variation of VFTO peak along the nodes of the GIS bus in the case of disconnector switch operation as compared to that of circuit breaker operation. It has also been noticed that the variation of VFTO peak levels are not in direct proportion to the trapped charge present on the HV bus.**

***Index Terms*—Disconnector switch, EMTP, gas insulated substation, trapped charge, very fast transient overvoltages.**

I. INTRODUCTION

IN GAS Insulated Substations (GIS), a large number of restrikes occur across the switching contacts when disconnector switch or circuit breaker is operated. Each strike leads to generation of a VFTO [1]. VFTO thus generated have rise-times in the range of a few ns and is followed by high frequency oscillations [2], [3]. Even though their magnitudes are lower than BIL of the system, they contribute to reduction in the life of insulation in the system due to their frequent occurrences. Also under VFTO, the dielectric strength of SF_6 in presence of free metallic particles is reduced considerably and may lead to flashover and thereby a ground fault [2]. VFTO can also influence the insulation of other GIS equipments such as transformers where the inter-turn insulation may be stressed with a higher voltage than under chopped lightning impulse voltages of same peak value [4], [5]. Hence, there is a need to estimate the magnitudes of VFTO generated during switching operations in GIS.

Since the VFTO magnitude depends on the location of the switching point, the substation layout as well as the magnitude of trapped charge on the HV bus, it is necessary to study their influence on the VFTO magnitudes.

II. COMPUTER SIMULATION

The fact that measurement of VFTO at such high frequencies is quite difficult and demands skill and utmost prudence, makes computer simulation of the above switching operations attractive. Also, simulation enables to estimate the VFTO magnitudes, their rise-times, effect on various components etc., with ease and reasonable accuracy even before the actual commissioning of the GIS.

A 420 kV GIS has been taken up for the simulation of VFTO during switching of various disconnectors and circuit breakers. A one line diagram of the 420 kV GIS is shown in Fig. 1. This substation has 4 main generators (G1 to G4) and 4 Auxillary generators (GA1 to GA4) feeding the three buses and there are three outgoing feeder lines from the substation. For the simulation work, the whole substation has been divided into three sections, *viz.*, the main generator lines, the auxillary generator lines and the outgoing feeder lines. Computer simulations have been done using EMTP software.

The Various Components of the 420 kV GIS and Their Equivalent Circuits

Since VFTO contain predominantly high frequency components ranging from hundreds of kHz to tens of MHz, most of the components have their capacitances dominating the other parameters [6].

The typical length of a GIS bus is much smaller than that of an ordinary substation and also, at high frequencies, in the range of few hundreds of kHz to MHz, the GIS bus acts like a transmission line with a finite transit time, propagation velocity and surge impedance. The value of surge impedance of GIS bus which is modeled as transmission line can be obtained from the relation.

$$Z = 60 \ln\left(\frac{b}{a}\right)\ \Omega \tag{1}$$

where, a is the diameter of the HV bus and b is the inner diameter of the enclosure. For the 420 kV GIS modeled, the surge impedance value is found to be 64.2 Ω [6].

Elbows, spacers and spherical shields are modeled by a lumped capacitance of 15 pF.

Power transformer with mounted bushing is modeled as lumped capacitance to ground of 1250 pF whereas surge arresters are modeled as lumped capacitance to ground of 50 pF [7].

Disconnector switches are modeled differently under open and closed conditions. When opened, they are modeled as two transmission lines in series with a capacitance. The surge impedance of each of the transmission lines is taken as 69 Ω and capacitance 20 pF. The capacitance to ground is taken as 52 pF.

When closed, the capacitance in between the two transmission lines of the open disconnector switch model is replaced by

Manuscript received March 16, 1999.

The authors are with the Department of High Voltage Engineering, Indian Institute of Science, Bangalore 560 012.

Publisher Item Identifier S 0885-8977(01)08515-6.

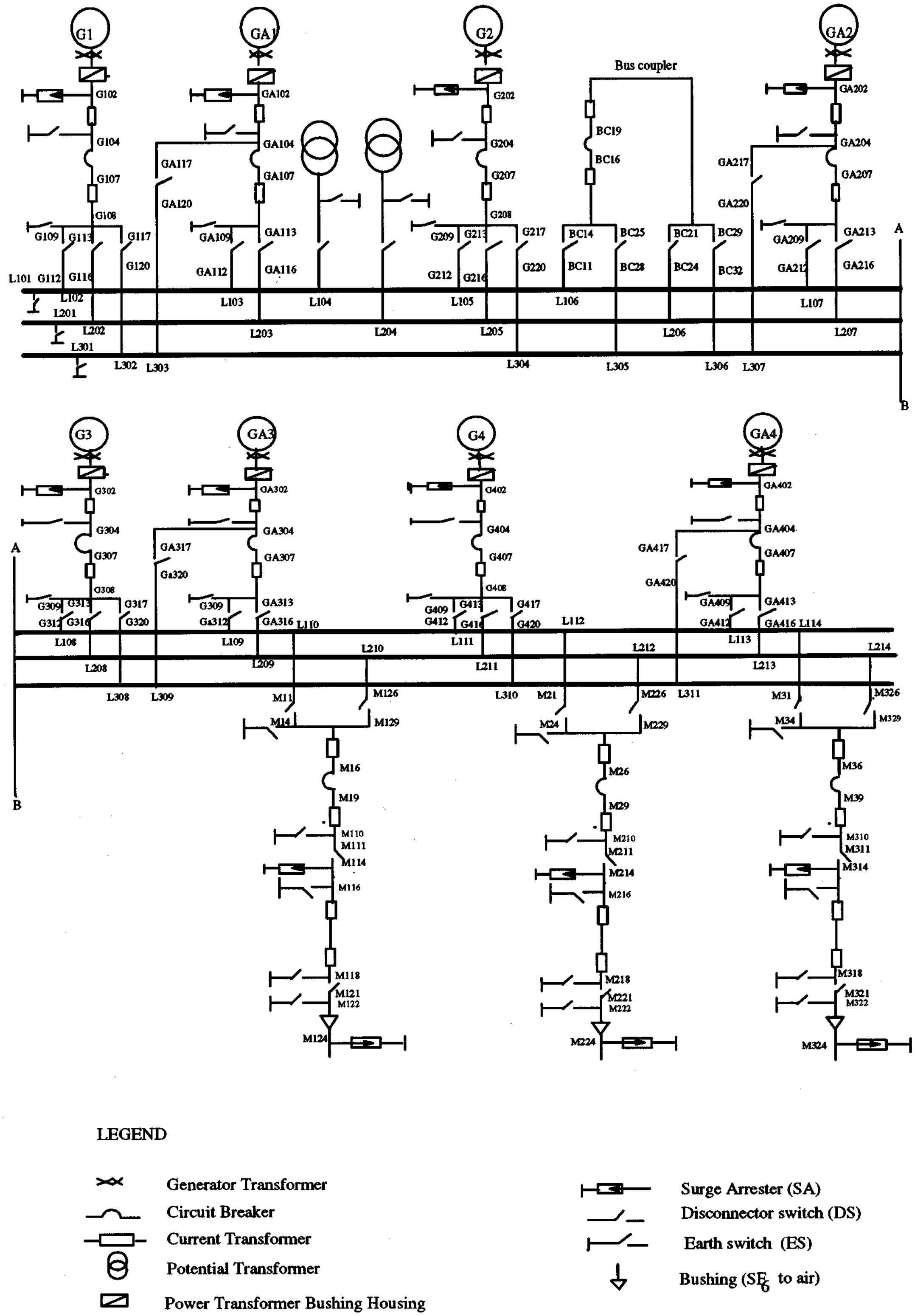

Fig. 1. Single line diagram of the 420 kV substation.

a transmission line with the same parameters as before but the capacitance to ground is taken as 88 pF.

The spark is modeled as an exponentially decaying resistance ($R_0e^{-t/T}$) in series with a small resistance (r) of 0.5 Ω to take care of the residual spark resistance. This is implemented using a piecewise nonlinear function in EMTP. The mathematical equation for the above is given by [6]

$$R = R_0e^{-(t/T)} + r. \tag{2}$$

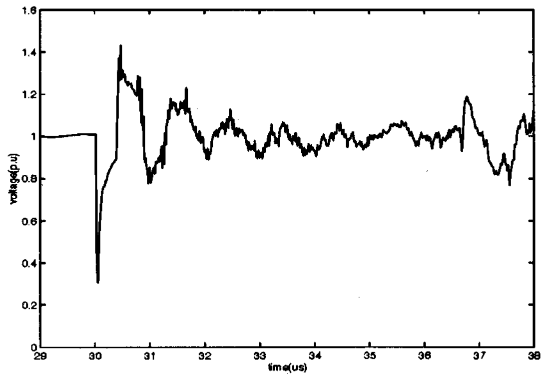

Fig. 2. VFTO waveforms for switching condition 1 at node M226.

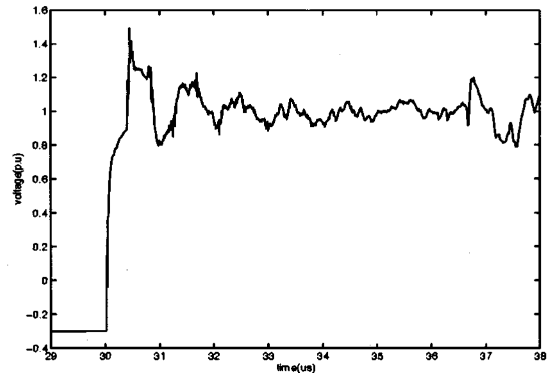

Fig. 3. VFTO waveforms for switching condition 1 at node M229.

R_0 is taken as 1×10^6 MΩ and T as 1 ns. The above equation gives a resistance whose value varies from very high value (MΩ) to a low value of 0.5 Ω within 30 ns.

Bushings are modeled with a lumped capacitance to ground of 500 pF whereas earth switches are modeled as lumped capacitances of 45 pF each.

Circuit breakers are also modeled differently under open and closed conditions. The open circuit breaker is modeled as two transmission lines in series with a capacitance of 2800 pF and a 17 Ω resistance in series between them. The capacitance to ground is taken as 200 pF. The closed circuit breaker is modeled similar to the open circuit breaker with the capacitance and resistance combination replaced by a transmission line having a surge impedance of 30 Ω. The capacitance to ground is also replaced by 20 pF.

The overhead line which is connected to the GIS is considered to be of infinite length. Hence, it is modeled as a transmission line terminated with a resistance to ground of value equal to the surge impedance of the overhead line (350 Ω), so that there is no reflection from this end.

III. Results and Discussion

Though simulation of 61 different switching conditions have been done for different trapped charge magnitudes of 0.3 p.u., 1.0 p.u. and 1.2 p.u., results of only two specific conditions have been presented and discussed here. The conditions considered are

1) All generators connected and the disconnector switch between M226 and M229 operated with circuit breaker between M26 and M29 kept open. A trapped charge of 1.0 p.u. is assumed on the HV bus.
2) All generators connected to the bus and the circuit breaker between M26 and M29 operated. A trapped charge of 1.2 p.u. is assumed on the HV bus.

VFTO Waveforms

The VFTO waveforms for the disconnector and circuit breaker switching conditions are shown in Figs. 2–5. VFTO waveforms have been computed for the same switching conditions at all the other GIS bus nodal points also. It has been observed that close to the switching point, VFTO waveform has steeper front and higher frequency of oscillation as compared to a farther away observation point.

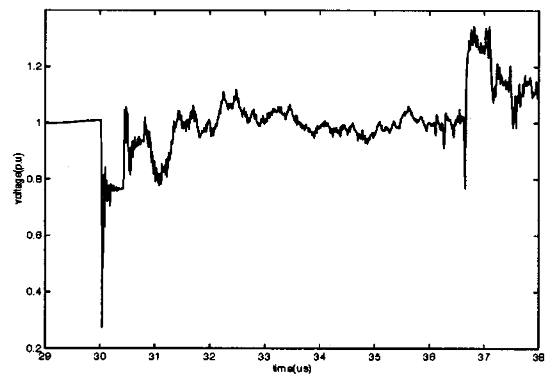

Fig. 4. VFTO waveforms for switching condition 2 at node M26.

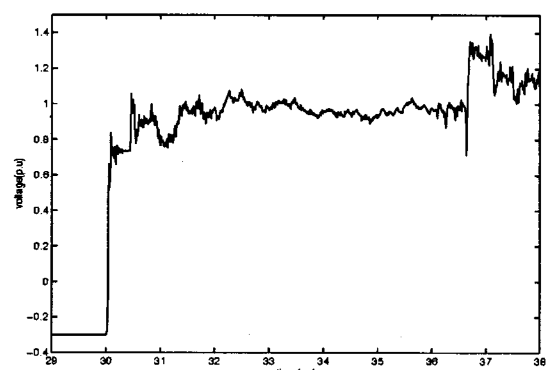

Fig. 5. VFTO waveforms for switching condition 2 at node M29.

Variation of VFTO Peak Along the Nodes

Fig. 6 shows the variation of the VFTO peak magnitudes along the nodes for disconnector switch operation, i.e., for condition no. 1.) Fig. 7 shows the variation of the VFTO peak magnitudes along the nodes for circuit breaker operation, i.e., for condition no. 2.)

In the case of disconnector switching operation (Fig. 6), the VFTO peak increases in the line where the switching is done (outgoing feeder line $X = 2$) till an open circuit breaker is encountered. Beyond this location, there is found to be a sharp reduction in the VFTO peak. The VFTO peak once again shows an increasing trend along the nodes and reaches a high value at the junction of the GIS with the overhead line. On the contrary, in the case of circuit breaker switching operation (Fig. 7), the VFTO peak has a steady increasing trend in the outgoing feeder

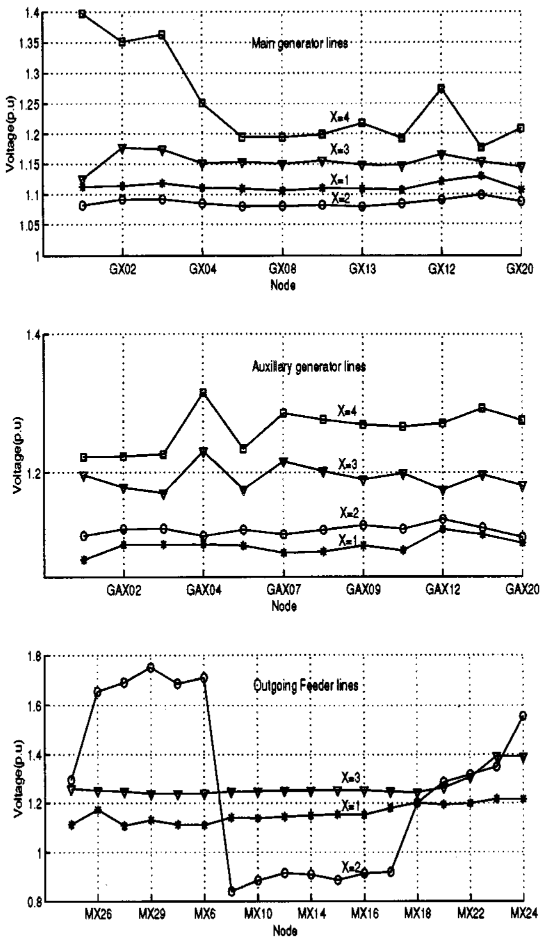

Fig. 6. Variation of VFTO levels for disconnector switch operation.

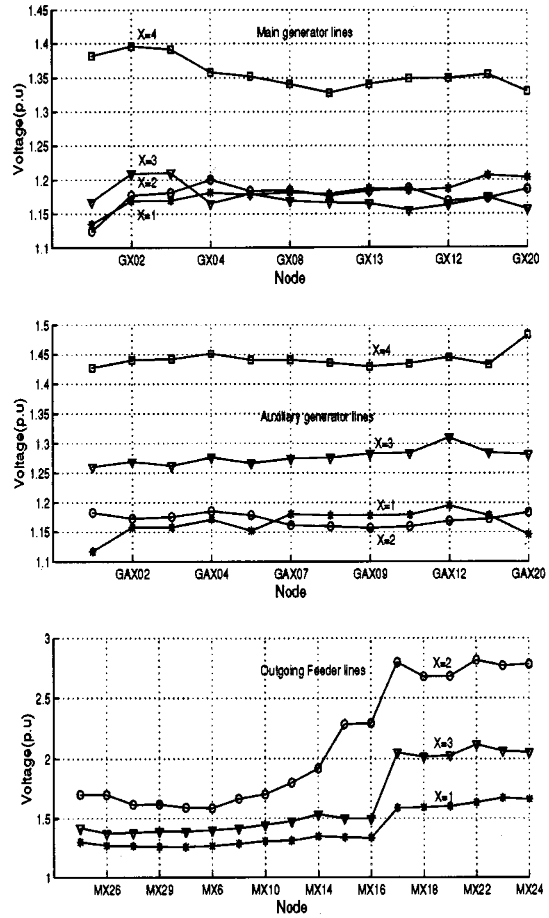

Fig. 7. Variation of VFTO levels for circuit breaker operation.

line (where the switching is done) till the junction of GIS with the overhead line. Also, it is found that the VFTO peak magnitudes are higher in the case of circuit breaker operation as compared to that of disconnector switching operation. It can also be observed that there is a distinct signature pattern of the peak VFTO magnitude variation for the disconnector switching operation as opposed to the circuit breaker switching operation along the outgoing feeder lines (where the switching has been done) as seen from Figs. 6 and 7. Similar patterns have been observed for all the switching conditions simulated. These signature patterns will be of use in determining the relative stress levels encountered by various GIS components for different switching conditions and for studying their long term aging behavior.

In the case of disconnector switching operation, VFTO peak is found to be highest when the disconnector switch between G320 and G317 is operated with the circuit breaker between G307 and G304 kept open and all the generators except G3 energized. Its value is 2.1 p.u. (node G305). In the case of circuit breaker operation, the VFTO peak magnitude is found to be maximum for circuit breaker between GA204 and GA207 operated and only GA2 line is connected and energized with a trapped charge of 1.2 p.u. Its value is 2.87 p.u. at the node M324 on the outgoing feeder $X = 3$.

It has been seen that VFTO peak magnitudes are higher close to the switching point for disconnector switching operations where as for circuit breaker operations maximum VFTO peak occur near the junction of GIS with the overhead line.

Effect of Trapped Charge on the VFTO Levels

The trapped charge left on a floating section of switchgear depends on the disconnector switch design and is usually less than 0.3 p.u. for a slow speed disconnector switch [8]. In the case of high speed disconnectors, the maximum trapped charge could be as high as 1.0 p.u. [9] whereas for circuit breakers it could be as high as 1.2 p.u. [10].

In order to understand the exact influence of the trapped charge on the VFTO levels, the variation of the VFTO magnitudes for the same switching case but for different trapped charge magnitudes, *viz.*, 1.0 p.u. and 0.3 p.u. were computed for disconnector switching operations. For circuit breaker switching operation, trapped charges of 1.2 p.u., 1.0 p.u. and 0.3 p.u. were used.

Fig. 8 shows the variation of the difference in VFTO peak along the nodes when the trapped charge is changed from 0.3 p.u. and 1.0 p.u. for the case wherein the disconnector switch between M226 and M229 is operated and the circuit breaker between M26 and M29 kept open with all the generators connected and energized. The variation is found to be the highest for the outgoing feeder line $X = 2$ whose value is 0.54 p.u. at the node M224 ($X = 2$). The maximum variation is 0.135 p.u. and 0.105 p.u. for the main generator lines G4

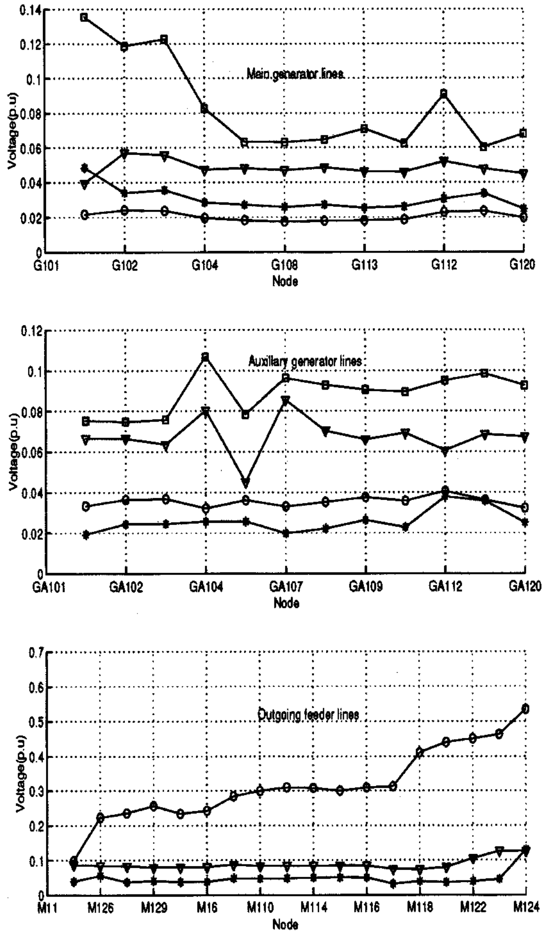

Fig. 8. Variation of difference in VFTO levels for disconnector switching operation.

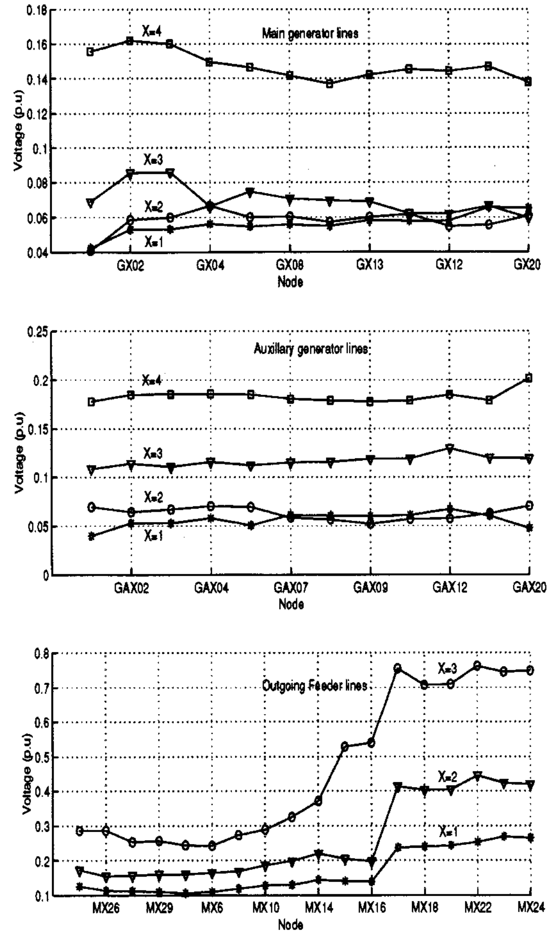

Fig. 9. Variation of difference in VFTO peak levels for circuit breaker operation.

(X = 4) and auxillary lines GA4 (X = 4), respectively. Even though, the trapped charge is increased by 0.7 p.u., the peak VFTO magnitude has increased by only 0.54 p.u. Similar trend is observed for other switching conditions also.

Fig. 9 shows the variation of the difference in VFTO peak along the nodes when the trapped charge is changed from 0.3 p.u. to 1.2 p.u. for the case wherein the circuit breaker between M26 and M29 is operated with all the generators connected and energized. The maximum variation of the VFTO peak levels in the outgoing feeder line is found to be close to 0.75 p.u. for the line M2 (X = 2) at the node M224. The maximum variation is 0.16 p.u. and 0.19 p.u. for main generator line (X = 4) and the auxillary generator line (X = 4), respectively.

It is found that the influence of trapped charge on VFTO magnitudes is more at the nodes in the line where the switching is done. It is also observed that the increase in peak VFTO magnitudes are not proportional to the increase in the trapped charge magnitude.

IV. Conclusion

The VFTO peak magnitudes are higher close to the switching point in the case of disconnector operations where as it is higher at the junction of the GIS with overhead line in the case of circuit breaker operation. Also, close to the switching point, VFTO waveform has steeper front time and higher frequency of oscillations as compared to a farther away observation point. There is also a distinct pattern of variation of VFTO peak along the nodes of the GIS in the case of disconnector switch operation as compared to that of circuit breaker operation. The circuit breaker operation results in the highest VFTO level amongst all the switching operations done.

When the trapped charge on the line is increased, there is an increase in the VFTO levels, but the increase is not proportional to the magnitude of the trapped charge. The influence of trapped charge on the VFTO magnitudes is more in the line where the switching is done. The variation of the difference in peak VFTO at different nodes have the same pattern as that of the plots showing the variation of VFTO peak magnitudes along the nodes for circuit breaker operation unlike for disconnector operation.

Acknowledgment

The authors thank the authorities of Indian Institute of Science for the permission to publish the paper. They are also indebted to the management of THDC for providing the layout of the GIS.

REFERENCES

[1] G. Ecklin, D. Schlicht, and A. Plessel, "Overvoltages in GIS caused by the operation of isolators," in *Surges in High Voltage Networks*, K. Ragaller, Ed. New York City: Plenum Press, 1980.

[2] Working Group 33/13-09, "Very fast transient phenomena associated with GIS," in *CIGRE*, 1988, paper 33-13, pp. 1–20.

[3] J. Meppelink, K. Diederich, K. Feser, and W. Pfaff, "Very fast transients in GIS," *IEEE Trans. Power Delivery*, vol. 4, no. 1, pp. 223–233, Jan. 1989.

[4] S. Fujita, N. Hosokawa, and Y. Shibyiya, "Experimental investigation of high frequency voltage oscillation in transformer winding," *IEEE Trans. Power Delivery*, vol. 13, no. 4, pp. 1201–1207, Oct. 1998.

[5] N. Fujimoto and S. A. Boggs, "Characteristics of GIS Disconnector-Induced Short Risetime Transients Incident on Externally Connected Power System Components,", vol. 3, July 1988.

[6] V. Vinod Kumar, "Estimation and measurement of very fast transient overvoltages (VFTO) in a gas insulated substation (GIS)," M.Sc.(Engg.) thesis, Indian Institute of Science, Bangalore, 1999.

[7] J. Lewis, B. M. Pryor, C. J. Jones, T. Irwin, L. C. Campbell, and A. Aked, "Disconnector operations in gas insulated substations overvoltage studies and tests associated with a 420 kV installation," in *CIGRE*, 1988, paper 33-09, pp. 0–8.

[8] S. A. Boggs, F. Y. Chu, and F. Y. Fujimoto, "Disconnect switch induced transients and trapped charge in Gas Insulated Substations," *IEEE Trans. Power Apparatus and Systems*, vol. PAS-101, no. 10, pp. 3539–3602, Oct. 1982.

[9] Task Force on Very Fast Transients, "Modeling and analysis guidelines for very fast transients," *IEEE Trans. Power Delivery*, vol. 11, no. 4, pp. 2028–2035, Oct. 1996.

[10] Joint Working Group, "Insulation co-ordination of GIS, return of experience on site tests and diagnostic techniques," *Electra*, no. 176, pp. 67–97, Feb. 1998.